Submitted to

XXII International Symposium on Lepton-Photon Interactions at High Energy, LP2005
June 30, 2005, Uppsala
Abstract: **390**
Session: **QCD and hadron structure**

www-h1.desy.de/h1/www/publications/conf/conf_list.html

Multi-jet production in high Q^2 neutral current deeply inelastic scattering at HERA and determination of α_s

H1 Collaboration

Abstract

Deep-inelastic e^+p scattering data, taken with the H1 detector at HERA, are used to investigate jet production over a range of four-momentum transfers $150 < Q^2 < 15000$ GeV^2 and transverse jet energies $5 < E_T < 50$ GeV. The analysis is based on data corresponding to an integrated luminosity of $\mathcal{L}_{int} = 65.4$ pb^{-1} taken in the years 1999-2000 at a centre-of-mass energy $\sqrt{s} = 319$ GeV. Jets are defined by the inclusive $k_\perp$ algorithm in the Breit frame of reference. Dijet and trijet cross sections are measured with respect to the exchanged boson virtuality and in addition the ratio of the trijet to the dijet cross section $R_{3/2}$ is investigated. The results are compared to the predictions of perturbative QCD calculations in next-to-leading order in the strong coupling α_s. The value of $\alpha_s(M_Z)$ determined from the study of $R_{3/2}$, is $\alpha_s(M_Z) = 0.1175 \pm 0.0017$ (stat.) $\pm\ 0.0050$ (syst.) $^{+0.0054}_{-0.0068}$ (th.).

1 Introduction

Deeply inelastic lepton-proton scattering (DIS) experiments have been vital to our understanding of the nature of the strong force. This has resulted in quantum chromodynamics (QCD) becoming established as the theory to describe the strong force in terms of interactions between quarks and gluons that carry different *colour* charges. QCD contains just one free parameter, the strong coupling α_s. The value of this coupling is known to run with the interaction energy scale and so α_s is usually quoted as its value at a scale that is very precisely known - the mass of the Z^0 boson. There are numerous experimental methods for the determination of α_s, for example by the consideration of fragmentation functions or by studying violations of Björken scaling. Furthermore, the production rates of DIS events containing more than one hard (high E_T) jet are directly sensitive to α_s[1]. By measuring the ratio of three and two jet event cross-sections ($R_{3/2}$), a value for α_s can be determined[2]. For this method of extracting α_s, precise values for both the inclusive dijet and trijet cross-sections are required. This document presents a measurement of the inclusive dijet and trijet cross-sections, as well as an extraction of α_s from a study of $\mathrm{R}_{3/2}$.

2 Theoretical Framework

2.1 The Breit Frame

This analysis has been conducted in the Breit inertial frame of reference[3]. The Breit frame is defined as the frame in which the exchanged boson is completely spacelike such that the relation $2x_{Bj}P^{\mu} + q = 0$ holds, where the incident proton four-vector is given by $P^{\mu} = (E_p, \mathbf{p_p})$ and q is the momentum transfer. The velocity of the Breit frame with respect to the laboratory frame is given by:

$$\beta = \frac{(\mathbf{q} + 2x_{Bj}\mathbf{p_p})}{(q_0 + 2x_{Bj}E_p)} \tag{1}$$

The fourvectors describing the DIS events are boosted and rotated such that the exchanged virtual boson is orientated along the negative z axis and such that the scattered lepton is directed in the positive x direction. It can be seen from the definition of the Breit frame that the transverse[1] energy of the hadronic final state does not have to balance the transverse energy of the scattered lepton, as is required in the laboratory frame. Instead, it directly reflects the hardness of the underlying QCD process. At lowest order the quark from the proton is backscattered and no transverse energy is produced. Jets with high E_T in this frame can only be accounted for by hard QCD processes whose contribution is at least $\mathcal{O}(\alpha_s)$ (figure 1)[4].

[1]Transverse refers to the component perpendicular to the z-axis.

3 Event Simulation

The order of magnitude and general features of the distributions for the jet cross-sections are well described by leading order (LO) calculations. More accurate predictions are required to include next-to-leading order (NLO) processes. Full NLO event simulations are not yet available for DIS events. An alternative method to obtain an approximation to higher order calculations is to use programs based on the parton cascade models. Programs such as RAPGAP[5], HERWIG[6] and LEPTO[7] contain additions to the LO matrix element based on soft and collinear emission approximations, described by parton shower models. The program ARIADNE[8] utilises the colour dipole model for these approximations. Programs to perform parton level cross-section calculations, at NLO, in DIS for jet multiplicities upto and including three jets are available and are employed in this study.

In this analysis the programs DJANGOH (version 1.2)[9] (used as an interface for ARIADNE) and RAPGAP (version 28) are utilised. These programs simulate the hard (DIS) scattering process for leptons on protons, and include first order QED radiative corrections (via the HERACLES program[10]) as well as initial and final state QCD radiation ($\mathcal{O}(\alpha_s)$). The parton density function (PDF) used in these programs is CTEQ5L. DJANGOH and RAPGAP account for the running of α_s to second order. The hadronisation of the final state following the breakup of the proton is not described by ARIADNE or RAPGAP. The hadronisation process is simulated using the Lund string fragmentation model[11] implemented in the program JETSET (version 7.4). Previous publications[12] have shown that the event generators used in this analysis provide an acceptable description of the internal structure of jets.

4 Event selection and jet search

The differential cross-sections presented in this report are given for the kinematic region defined by $150 < Q^2 < 15000\ GeV^2$ and $0.2 < y < 0.6$.

4.1 Data sample

The data sample was collected with the H1 detector during the 1999-2000 e^+p data taking period at HERA and corresponds to an integrated luminosity of 65.4 pb^{-1}. The events chosen for this analysis are characterised by a high-energy isolated positron in the central region of the detector. The event selection criteria closely follow that used in recent measurements of the inclusive DIS cross-section[13], the dijet cross section[14] and the trijet cross section[15]. The variables Q^2, x_{Bj} and y were determined using the electron-sigma method [16].

4.2 Jet search

The inclusive $k_\perp$-cluster algorithm was used to reconstruct jets in both data and simulated events. The algorithm is defined by a radius parameter R_o, which defines the minimal separation of jets in pseudorapidity[2] and azimuth space. R_o was set to unity as in [17]. A complete description of the inclusive $k_\perp$-clustering algorithm can be found in [14, 17].

Only jets with $E_T > 5$ GeV are considered for the jet cross section measurements. Jets must also fall within the pseudorapidity range $-1 < \eta_{Lab}^{jet} < 2.5$. In order to reduce infrared sensitive regions of phase space, and thus ensure the stability of the NLO calculations, events considered for the trijet (dijet) cross section are included only if the three (two) jets of highest E_T have an invariant mass $M_{3jet} > 25$ GeV ($M_{2jet} > 25$ GeV).

The range of the inelasticity variable, y, was chosen to exclude regions with large x_{Bj} (where jets tend to be produced in the forward direction, at the edge of detector acceptance) and to ensure large energies of the scattered positron respectively. In this document the proton remnant is not included in the jet count and is neglected.

After all cuts have been made a total of 5460 dijet events and 1757 trijet events remained.

5 Correction Procedure

The data are corrected for limiting features of the detector, such as resolution and acceptance. Samples of simulated events were created using the generators ARIADNE, which is implemented via the DJANGOH program (version 1.2), and RAPGAP (version 28). Both DJANGOH and RAPGAP provide a good description of the distributions of the experimental data for the DIS, dijet and trijet samples[3] (figures 2 - 4) and so the weighted average of the correction factors from both simulations were utilised in the correction procedure.

The correction functions are determined on a bin-by-bin basis as the ratio of the value of the generator and reconstructed level sets. It was found that the values of the correction functions are typically ~ 1.10 for dijet events and ~ 0.95 for trijet events The ratio of generator level events without QED radiation to those with, yields QED correction factors that are typically ~ 1.05 for dijet and trijet events.

6 NLO Predictions

There are several programs available to perform dijet cross-section calculations in next-to-leading order. DISENT[18], and DISASTER have been used in many previous analyses

[2]Pseudorapidity is defined as $\eta = -ln(tan\frac{\theta}{2})$ where θ is the polar angle.
[3]The jet samples from RAPGAP require an aditional renormalisation factor of ~ 1.2.

and provide consistent results[19]. However, only NLOJET++ allows the three jet cross-section from ep collisions to be calculated to NLO. NLOJET++ has been shown to be consistent with both DISENT and DISASTER for the dijet cross-section at LO and NLO[15, 20].

For the region of Q^2 considered in this analysis, it has been shown that there is little difference in the size of the NLO corrections to the born level, for dijets, between the choice of Q^2 or $\overline{E}_T^2$[4] for the renormalisation/factorisation scale used in the NLO calculations[14]. It has been observed that the choice of Q^2 produces marginally smaller scale uncertainty for the value of $R_{3/2}$ and so this has been used for the renormalisation/factorisation scale in this analysis. Values for the k-factor, which represents the size of the NLO correction to the born level, for dijets are $\sim$ 1.2 - 1.05 and for trijets are $\sim$ 1.25 (figure 5).

The NLO predictions use the $\overline{MS}$ scheme for five massless quark flavours. The parton distribution function (PDF) used in this analysis for comparison with data is CTEQ5M (the CTEQ4A[21] PDF is also employed for the QCD analysis). The value of $\alpha_s(M_Z)$ used with this PDF was $\alpha_s(M_Z) = 0.118$, and this value was subsequently evolved according to the two-loop solution of the renormalisation group equation. NLOJET++ produces cross-sections at the parton level and as such requires a correction for hadronisation effects before a comparison with data can be made. This was performed bin-by-bin, where hadronisation correction factors C_{had} were defined as the ratio of the hadron-to-parton level cross-sections and were taken to be the average of values found using the programs DJANGOH and RAPGAP. The hadronisation correction factors were typically ~ 0.93 for dijets and ~ 0.75 for trijets

The influence of heavy quark masses and electroweak effects are not included in the calculations from NLOJET++. It has been shown that at LO these effects are small ($< 1\%$) for the kinematic region considered in this analysis, with the exception of the highest Q^2 bin ($5000 < Q^2 < 15000$ GeV^2), where the expected change in the dijet cross-section is $\sim 25\%$. For this reason, this bin is not used in the QCD analysis presented in this document. It may be possible to include this region at a future time using an electroweak correction procedure, using a method similar to that employed for detector, QED and hadronisation corrections.

7 Systematic and theoretical uncertainties

The effect of several sources of systematic uncertainties are considered.

- The calibration of the positron energy is varied by $\pm$ (0.7-3)%, depending on the position of the positron within the detector
- The positron polar angle is varied by $\pm$ 1-3 mrad, depending on the position of the positron within the detector

[4]Mean E_T of the leading jets

- The positron azimuthal angle is varied by ± 3 mrad
- An overall hadronic uncertainty of 2% is taken into account by shifts up and down of the hadronic energy scale of the H1 calorimeters as well as the track momenta of the hadronic final state.
- The difference between using the average correction factor and that of DJANGOH or RAPGAP alone as an estimate of the model uncertainty
- The uncertainty due to the measurement of the luminosity is also considered

The systematic uncertainties are combined in quadrature with the statistical uncertainties of the data and the correction function to produce a total estimation of the error on the measurement of the cross-sections.

The main contributions to the uncertainty associated with the theoretical cross-section predictions are:

- Uncertainties due to the hadronisation correction factor, estimated as the difference between using the average correction factor and that of DJANGOH or RAPGAP alone
- Uncertainties due to terms beyond NLO and the choice of scale, estimated by varying the renormalisation/factorisation scale by a factor of two

The total theoretical uncertainty was obtained by adding the individual contributions in quadrature.

8 Experimental Results

8.1 Cross-sections

Values for the inclusive dijet and trijet cross-sections show good agreement with published measurements [14, 15], taking into account slight differences due to the increase in the HERA beam energy. Owing to the size of the dataset employed in this study, the range of Q^2 has been extended compared with existing three jet studies[15]. The highest Q^2 point has large statistical uncertainties due to the low event rate in this kinematic region, but represents the first measurement of the three jet cross-section in this kinematic region for *ep* collisions. The cross-sections show good agreement with the predictions of NLOJET++ in the phasespace region where electroweak effects can be neglected (figures 6,7).

8.2 $R_{3/2}$ and determination of α_s

The distribution of $R_{3/2}$ with respect to Q^2 is well described by the NLO predictions in the region where electroweak effects can be neglected. Data lie within one standard deviation of the central NLO prediction, and well within the theoretical uncertainty associated with the renormalisation/factorisation scale, across almost two orders of magnitude in Q^2 (figure 8). Many systematic uncertainties cancel in the ratio as a large proportion of the trijet sample is contained within the dijet sample.

The distribution of $R_{3/2}$ with respect to Q^2, excluding the final Q^2 bin, was used to extract $\alpha_s(M_Z)$. The PDF CTEQ4A provides PDF sets obtained with different $\alpha_s(M_Z)$ values[5]. It has been shown to be consistent with the CTEQ5 PDFs for the Q^2 range considered in this analysis. The method for extraction is similar to that employed in a recent publication by the ZEUS collaboration[2]. The procedure is as follows:

- The NLO calcultions are repeated for each available value of $\alpha_s(M_Z)$.
- The function $C_1\alpha_s(M_Z) + C_2\alpha_s^2(M_Z)$ is fitted to the theoretical predictions from NLOJET++ using the CTEQ4A PDF, for each bin in Q^2.
- A value of $\alpha_s(M_Z)$ is determined for each bin in Q^2 and an overall value calculated using a χ^2 minimisation over the entire Q^2 range.

Taking into account only the statistical uncertainties on the measured values of $R_{3/2}$, $\alpha_s(M_Z)$ is determined to be $\alpha_s(M_Z) = 0.1175 \pm 0.0017$ (stat.)

The systematic and theoretical uncertainties of the extracted value of the strong coupling are found by repeating the above procedure using the cross-sections shifted by the total systematic and theoretical uncertainties as described above. The value of $\alpha_s(M_Z)$ extracted from $R_{3/2}$ is thus:

$$\alpha_s(M_Z) = 0.1175 \pm 0.0017\ (\text{stat.}) \pm 0.0050\ (\text{syst.})\ ^{+0.0054}_{-0.0068}\ (\text{th.}).$$

This result is in good agreement with the current world average (figure 9) and with the evolution of α_s predicted by pQCD (figure 10). The value is competitive with results from other experimental procedures from different processes and is in agreement with the result recently obtained from $R_{3/2}$ by the ZEUS collaboration[2].

9 Summary

Differential cross-sections, with respect to Q^2, have been measured for dijets and trijets in neutral current DIS for $150 < Q^2 < 15000$ GeV^2 at HERA using the H1 detector. The ratio $R_{3/2}$ of the trijet to the dijet cross-section has been measured as a function of

[5] $\alpha_s(M_Z)$ values available in the CTEQ4A PDF are 0.110, 0.113, 0.116, 0.119 and 0.122

Q^2. NLO pQCD predictions provide a good description of the cross-sections and $R_{3/2}$ in the phasespace region where electroweak effects can be neglected. $\alpha_s(M_Z)$ is extracted using the distribution of $R_{3/2}$ for $150 < Q^2 < 5000\mathrm{GeV}^2$, with the value of the strong coupling, at the mass of the Z boson, found to be $\alpha_s(M_Z) = 0.1175 \pm 0.0017$ (stat.) $\pm$ 0.0050 (syst.) $^{+0.0054}_{-0.0068}$ (th.) in good agreement with the current world average and previous HERA results.

10 Acknowledgements

We are grateful to the HERA machine group whose outstanding efforts have made and continue to make this experiment possible. We thank the engineers and technicians for their work in constructing and now maintaining the H1 detector, our funding agencies for financial support, the DESY technical staff for continual assistance, and the DESY directorate for the hospitality which they extend to the non DESY members of the collaboration.

11 References

References

[1] H1 Collaboration, S. Aid et al., Nucl. Phys. B 449 (1995) 3;
ZEUS Collaboration, M. Derrick et al., Phys. Lett. B 363 (1995) 201;
H1 Collaboration, C. Adloff et al., Eur. Phys. J. C5 (1998) 625;
H1 Collaboration, C. Adloff et al., Eur Phys. J. C6 (1999) 575.

[2] ZEUS Collaboration, S. Chekanov et al., hep-ex/0502007 (2005)

[3] R.P. Feynman, "Photon-Hadron Interactions"[Benjamin, NY (1972)]
K.H.Streng, T.F.Walsh, P.M. Zerwas, Z. Phys. C 2, 237 (1979).

[4] B.R. Webber, J. Phys. G19 (1993) 1567.

[5] H. Jung, Comp. Phys. Comm. 86 (1995) 147.

[6] G. Marchesini et al., Comp. Phys. Comm. 67 (1992) 465.

[7] G. Ingelman, A. Edin and J. Rathsman, Comp Phys. Comm, 101 (1997) 108.

[8] L. Lönnblad, Comp. Phys. Comm. 71 (1992) 15.

[9] K. Charchula, G. Schuler and H. Spiesberger, Comp. Phys. Comm. 81 (1994) 381.

[10] A. Kwiatkowski, H. Spiesberger and H-J. Möhring, Comp. Phys. Comm. 69, 155 (1992)

[11] B. Andersson et al., Phys. Rep 97 (1983) 31.

[12] H1 Collaboration, C. Adloff et al., Nucl. Phys. B 545 (1999) 3.

[13] H1 Collaboration, C. Adloff et al., Eur. Phys. J. C 13 (2000) 609.

[14] H1 Collaboration, C. Adloff et al., hep-ex/0010054v1 (2000)

[15] H1 Collaboration, C. Adloff et al., Phys. Lett. B515 (2001) 17-29.

[16] U. Bassler and G. Bernardi, Nucl. Instr. Meth. A 426 (1999) 583.

[17] S.D. Ellis and D.E. Soper, Phys. Rev. D 48 (1993) 3160;
S. Catani, Yu.L. Dokshitzer, M.H. Seymour and B.R. Webber, Nucl. Phys. B 406 (1993) 187.

[18] S. Cantani and M.H. Seymour, Nucl. Phys. B 485 (1997) 291, Erratum-ibid. B 510 (1997) 503.

[19] C. Duprel, Th. Hadig, N. Kauer and M. Wobisch, Proceedings of the HERA Monte Carlo Workshop, eds. G. Grindhammer, G. Ingelman, H. Jung, T. Doyle, DESY-PROC-02-1999 (1999) 142.

[20] Z. Nagy and Z. Trocsanyi, Phys. Rev. Lett. 87 (2001) 082001.

[21] H.L. Lai et al., Phys. Rev. D. 55 (1997) 1280.

[22] Particle Data Group, S. Eitelman et al., Phys. Lett. B 592 (2004) 1.

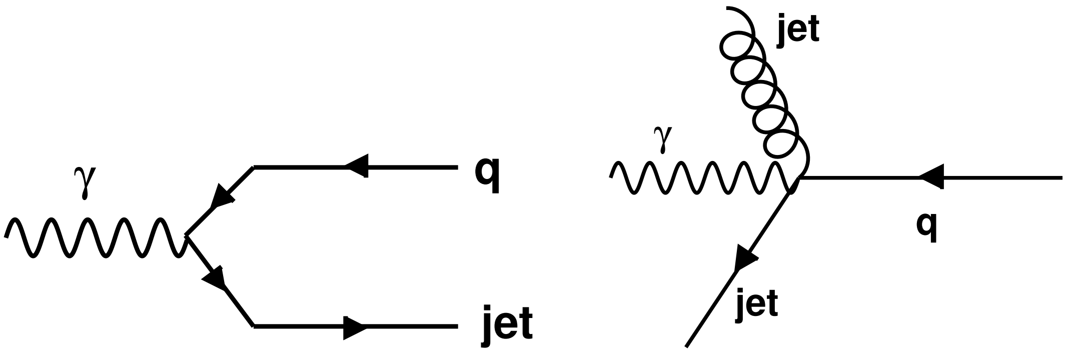

Figure 1: Diagrams showing lowest order (left) and high E_T (right) jet events in the Breit frame[14].

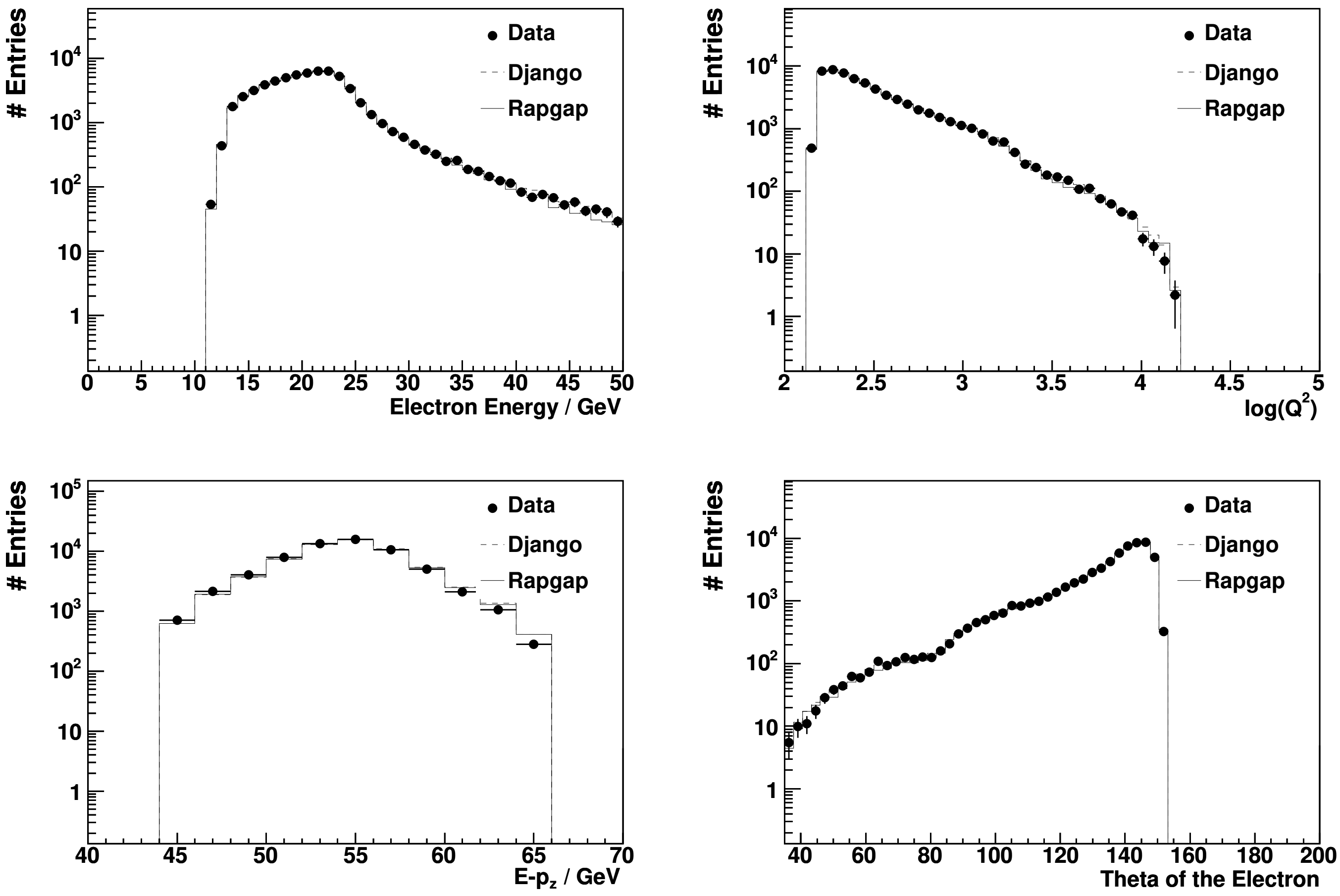

Figure 2: Control distributions for the DIS event sample. Distributions are normalised to equal number of events and show comparison of data (points) with RAPGAP (solid line) and DJANGOH (dashed line). Plots are energy of scattered positron (GeV) (top left), $\log_{10}(Q^2)$ (top right), E-P_Z (GeV) (bottom left) and polar angle of the scattered positron (degrees) (bottom right).

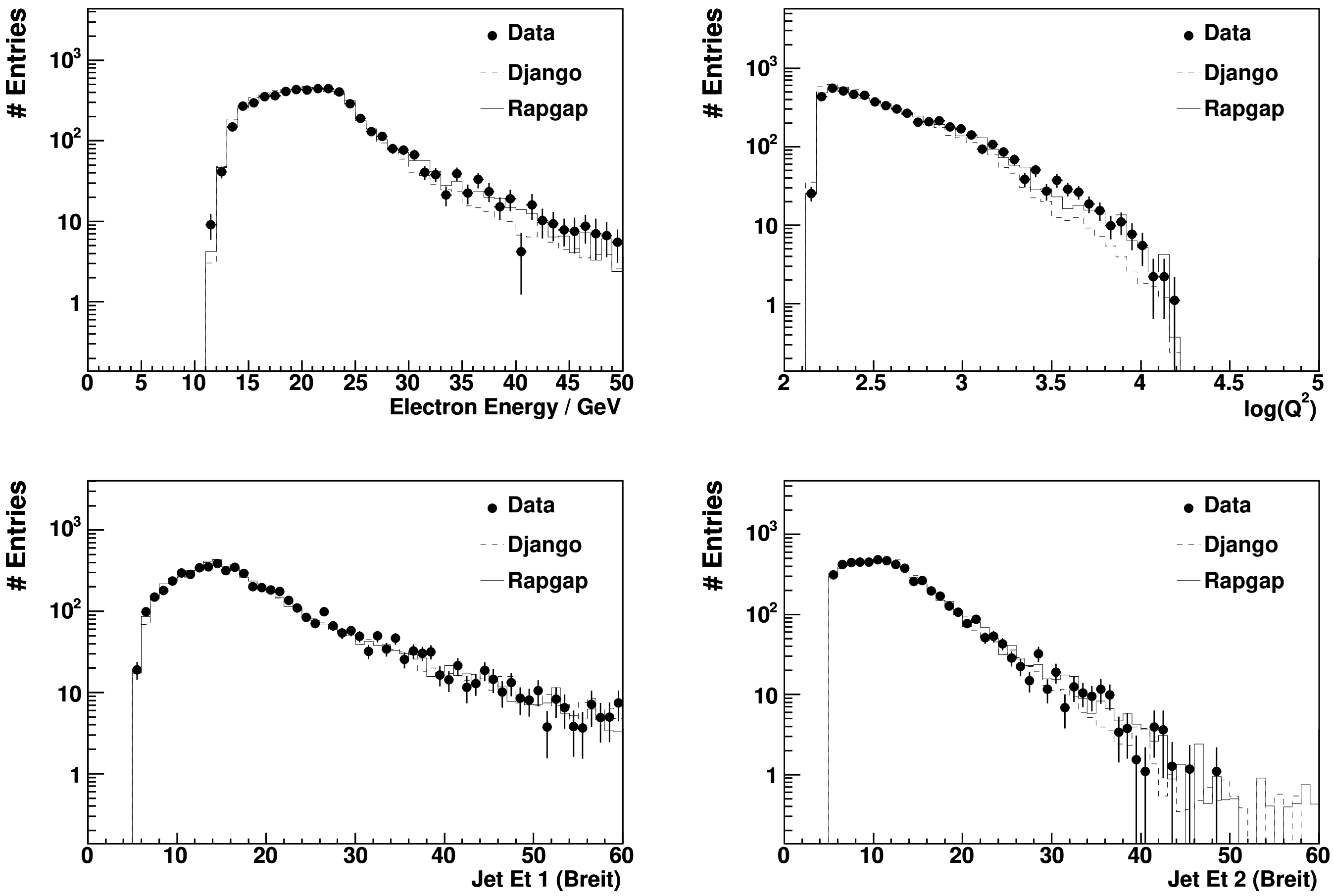

Figure 3: Control distributions for the diijet event sample. Distributions are normalised to equal number of events and show comparison of data (points) with RAPGAP (solid line) and DJANGOH (dashed line). Plots are energy of scattered positron (GeV) (top left), $\log_{10}(Q^2)$ (top right), E_T of highest E_T jet (GeV) (bottom left) and E_T of second highest E_T jet (GeV) (bottom right).

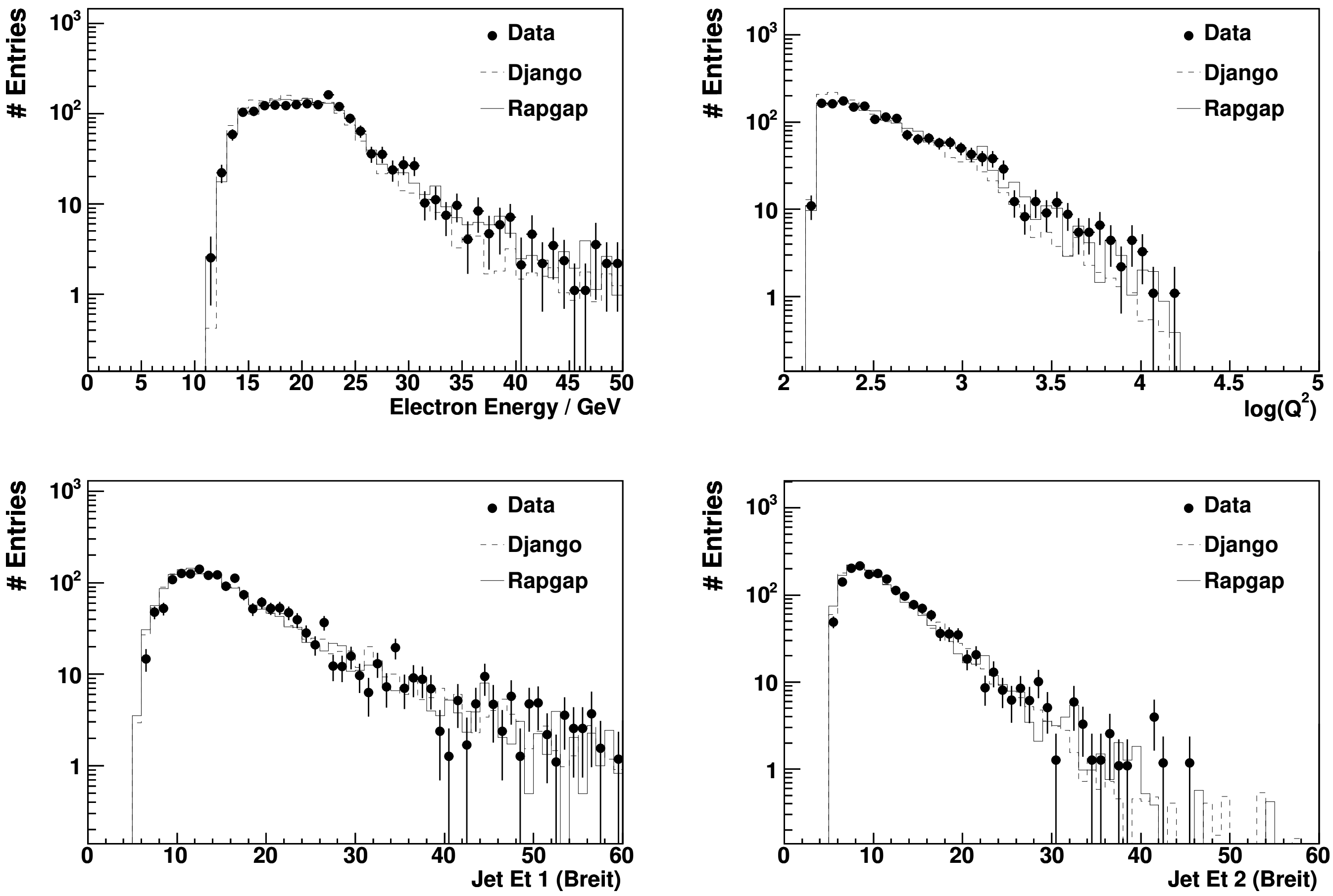

Figure 4: Control distributions for the trijet event sample. Distributions are normalised to equal number of events and show comparison of data (points) with RAPGAP (solid line) and DJANGOH (dashed line). Plots are energy of scattered positron (GeV) (top left), $\log_{10}(Q^2)$ (top right), E_T of highest E_T jet (GeV) (bottom left) and E_T of second highest E_T jet (GeV) (bottom right).

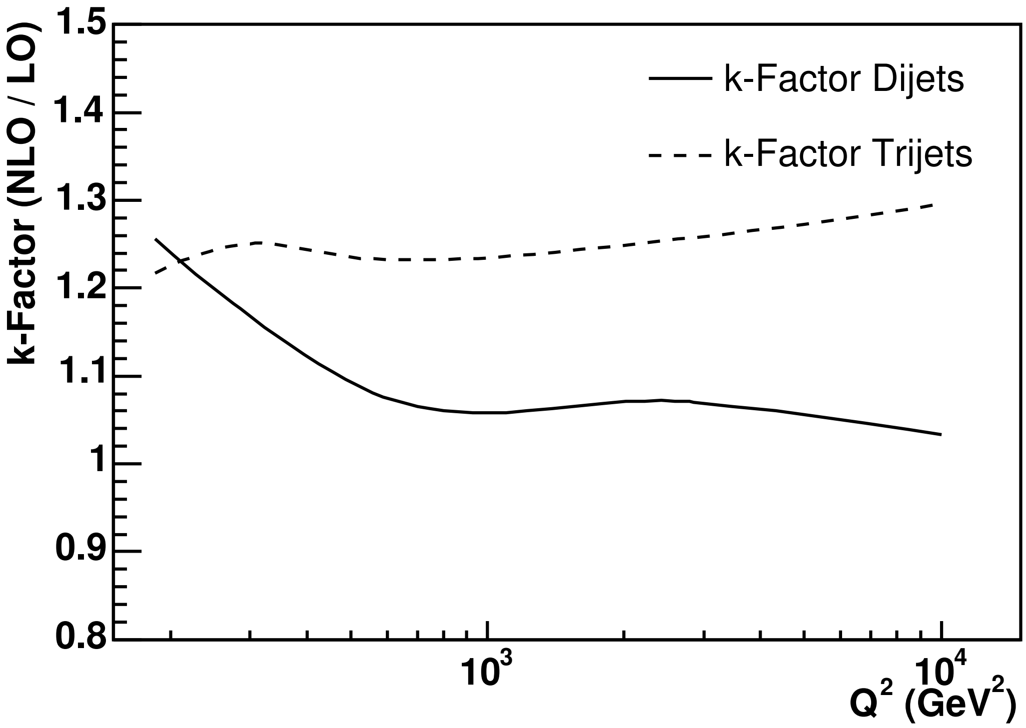

Figure 5: k-Factors for dijets (solid line) and trijets (dashed line). Q^2 is used as the choice of renormalisation/factorisation scale.

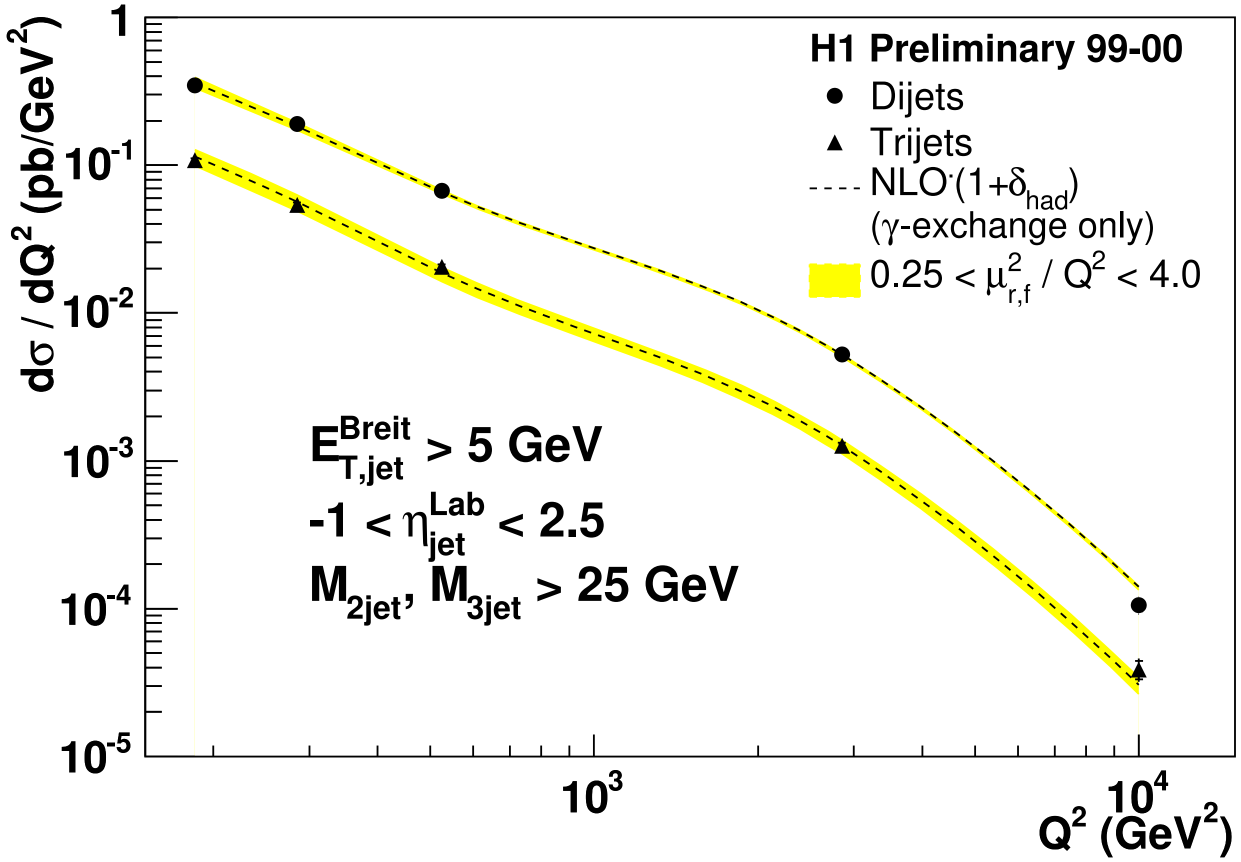

Figure 6: NC dijet and trijet differential cross-sections, with respect to Q^2, shown with NLO pQCD predictions including hadronisation corrections. The shaded bands show the effect of varying the renormalisation/factorisation scale by a factor of two. The highest Q^2 bin is overestimated by the theoretical predictions due to the absence of electroweak effects in the NLO calculations.

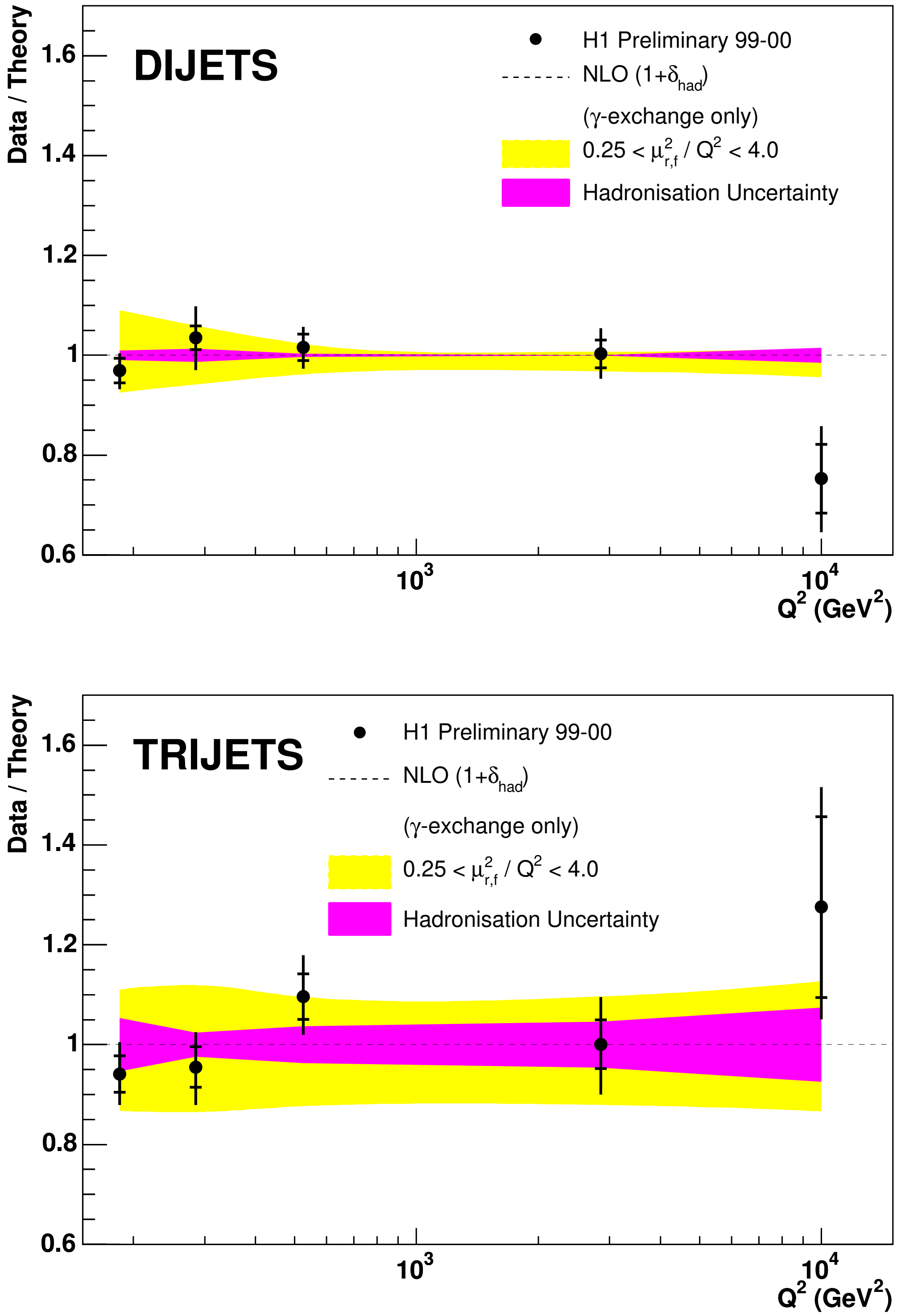

Figure 7: Ratio of dijet (top) and trijet (bottom) differential cross-sections, to NLO predictions (including hadronisation corrections). The light shaded bands show the effect of varying the renormalisation/factorisation scale by a factor of two. The dark shaded bands show the uncertainty associated with the hadronisation correction.

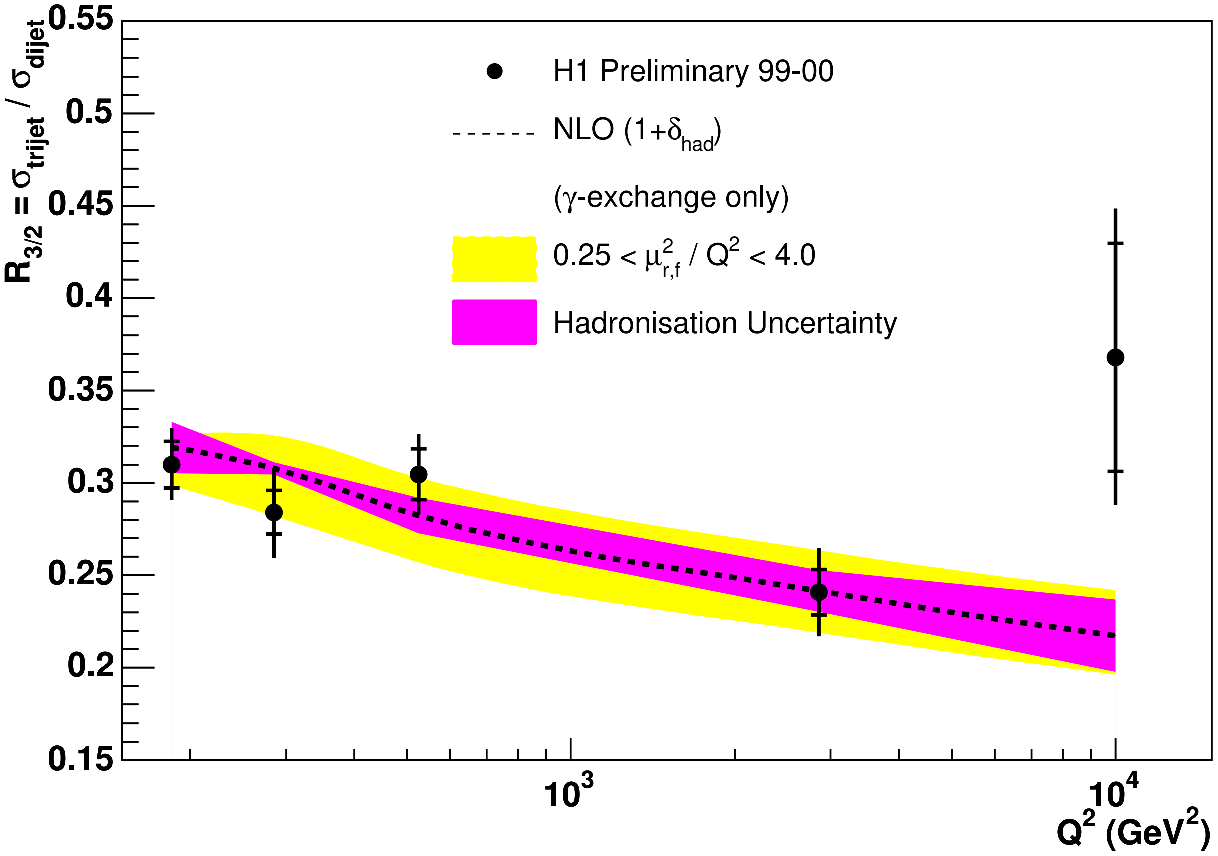

Figure 8: Distribution of measured values of $R_{3/2}$ against Q^2 compared with a NLO pQCD prediction, with hadronisation corrections. The light shaded band shows the effect of varying the renormalisation/factorisation scale by a factor of two. The dark shaded band shows the uncertainty associated with the hadronisation correction.

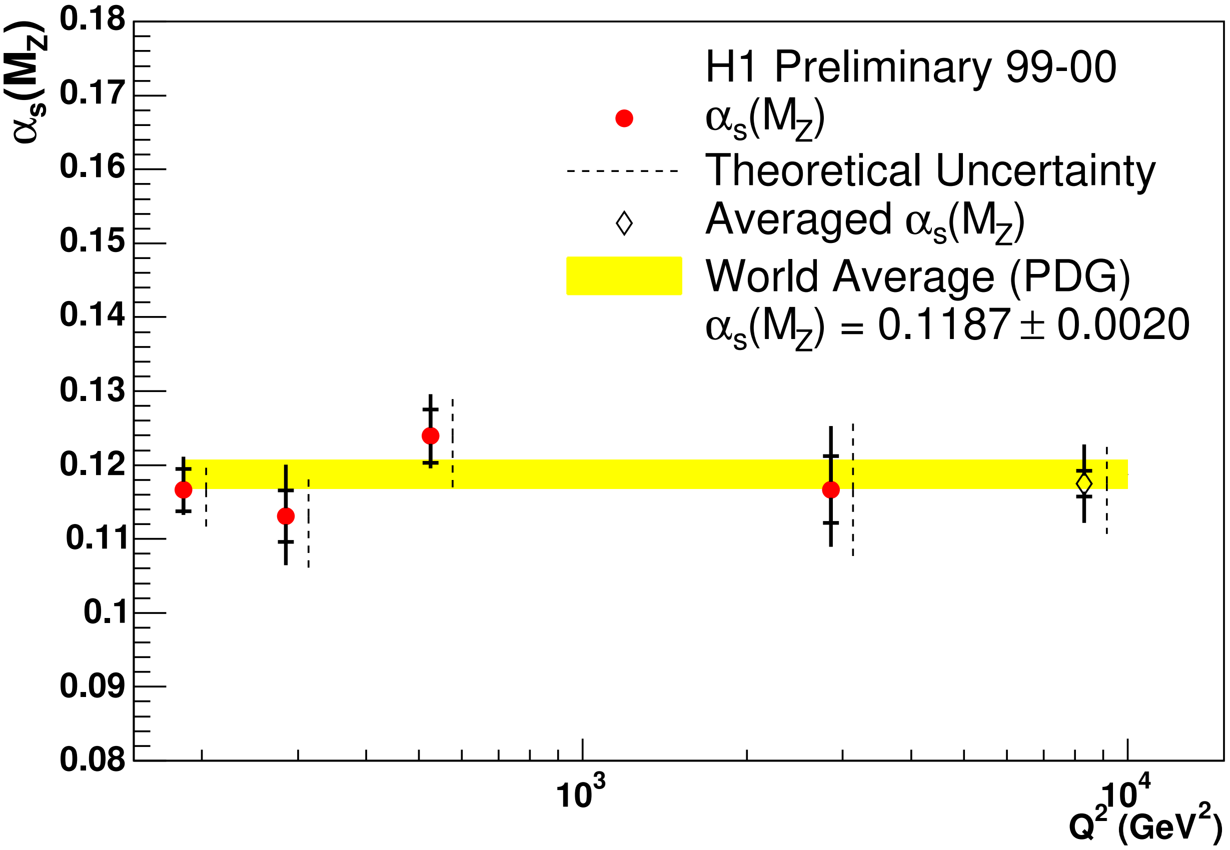

Figure 9: $\alpha_s(M_Z)$ values from each Q^2 bin. The averaged value, found using a χ^2 minimisation fit, is shown at the far right (empty diamond) and is disassociated with the x-axis. Uncertainties shown are statistical up to the horizontal bar, and then the quadratic sum of statistical and systematic uncertainties. Theoretical uncertainties, associated with the extraction of α_s, are offset right. The world average is $\alpha_s(M_Z) = 0.1187 \pm 0.0020$.

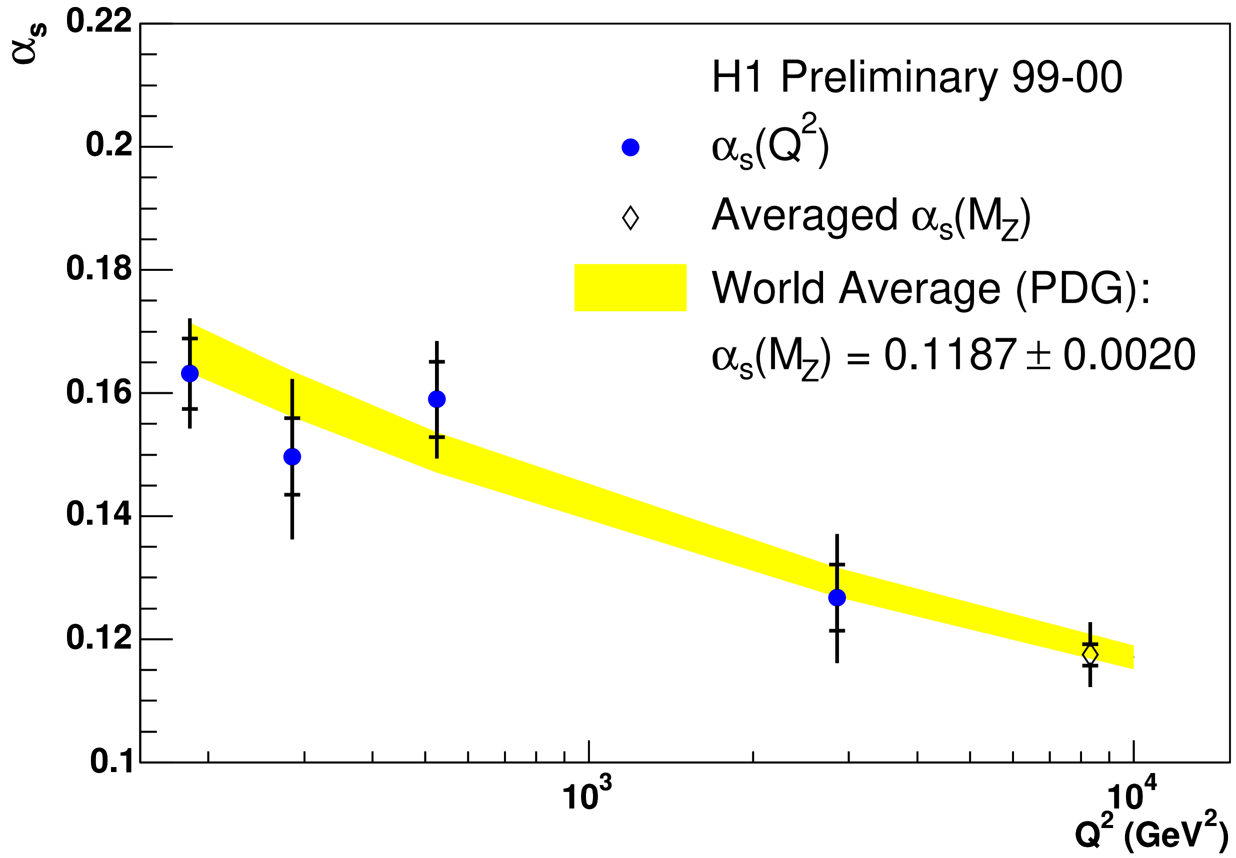

Figure 10: $\alpha_s(M_Z)$ values from each Q^2 bin evolved to their values at their respective values of Q^2 (triangles) using the two-loop solution of the renormalisation group equation. The averaged value of $\alpha_s(M_Z)$, found using a χ^2 minimisation fit, is shown at the far right (empty diamond). The evolution of the current world average value of $\alpha_s(M_Z)$ is shown as a shaded band. Uncertainties shown are statistical up to the horizontal bar, and then the quadratic sum of statistical and systematic uncertainties. . The world average is $\alpha_s(M_Z)$ = 0.1187 ±0.0020.